DOI:
10.1021/acsami.7b08473

Document Version
Peer reviewed version

ACS APPLIED MATERIALS & INTERFACES

Article

Post-Polymerization C-H Borylation of Donor-Acceptor Materials Gives Highly Efficient Solid State Near-Infrared Emitters for NIR-OLEDs and Effective Biological Imaging

Daniel L. Crossley, Laura Urbano, Robert Neumann, Struan Bourke, Jennifer Jones, Lea Ann Dailey, Mark A Green, Martin Humphries, Simon M King, Michael L Turner, and Michael J. Ingleson

ACS Appl. Mater. Interfaces, **Just Accepted Manuscript** • DOI: 10.1021/acsami.7b08473 • Publication Date (Web): 07 Aug 2017

ACS Publications

ACS Applied Materials & Interfaces is published by the American Chemical Society. 1155 Sixteenth Street N.W., Washington, DC 20036

Post-Polymerization C-H Borylation of Donor-Acceptor Materials Gives Highly Efficient Solid State Near-Infrared Emitters for NIR-OLEDs and Effective Biological Imaging

Daniel L. Crossley[†], Laura Urbano[‡], Robert Neumann[§], Struan Bourke[∥], Jennifer Jones[†], Lea Ann Dailey*[§], Mark Green[∥], Martin J. Humphries[⊥], Simon M. King[⊥], Michael L. Turner*[†], Michael J. Ingleson*[†].

[†]School of Chemistry, University of Manchester, Manchester, M13 9PL, UK.

[‡]King's College London, Institute of Pharmaceutical Sciences, Waterloo Campus, SE1 9NH London (UK)

[§]Institute of Pharmacy, Martin-Luther University Halle-Wittenberg, Wolfgang-Langenbeck-Str. 4, 06120 Halle (Saale), Germany

[∥]King's College London, Department of Physics, Strand Campus, WC2R 2LS London, UK.

[⊥]Cambridge Display Technology Limited (Company Number 02672530), Unit 12, Cardinal Park, Cardinal Way, Godmanchester, PE29 2XG, UK.

KEYWORDS: *near-infrared emission, bioimaging, post-polymerization modification, C-H borylation, low band-gap.*

ABSTRACT: Post-polymerization modification of the donor-acceptor polymer, poly(9,9-dioctylfluorene-alt-benzothiadiazole), PF8-BT by electrophilic C-H borylation is a simple method to introduce controllable quantities of near-infrared (NIR) emitting chromophore units into the backbone of a conjugated polymer. The highly stable borylated unit possesses a significantly lower LUMO energy than the pristine polymer resulting in a reduction in the band-gap of the polymer by up to 0.63 eV and a red shift in emission of more than 150 nm. Extensively borylated polymers absorb strongly in the deep red / NIR and are highly emissive in the NIR region of the spectrum in solution and solid state. Photoluminescence quantum yields (PLQY) values are extremely high in the solid state for materials with emission maxima ≥ 700 nm with PLQY values of 44% at 700 nm and 11% at 757 nm for PF8-BT with different borylation levels. This high brightness enables efficient solution processed NIR emitting OLEDs to be fabricated and highly emissive borylated polymer loaded conjugated polymer nanoparticles (CPNPs) to be prepared. The latter are bright, photo-stable, low toxicity bio-imaging agents that in phantom mouse studies show higher signal to background ratios for emission at 820 nm than the ubiquitous NIR emissive bioimaging agent indocyanine green. This methodology represents a general approach for the post-polymerization functionalization of donor acceptor polymers to reduce the band gap as confirmed by the C-H borylation of poly((9,9-dioctylfluorene)-2,7-diyl-alt-[4,7-bis(3-hexylthien-5-yl)-2,1,3-benzothiadiazole]-2c,2cc-diyl) (PF8TBT) resulting in a red-shift in emission of > 150 nm thereby shifting the emission maximum to 810 nm.

INTRODUCTION

The development of organic materials that are effective solid state near-infrared (NIR) emitters is of considerable significance for many applications including night-vision displays, sensors and in-vivo fluorescence imaging.[1,2] The latter is particularly important as it is a non-invasive diagnosis method that provides information not available by in-vitro or ex-vivo imaging.[3-5] However, efficient solid state NIR emission is challenging as organic materials that demonstrate substantial NIR emission (>700 nm) in solution often show severely decreased photoluminescence quantum yield (PLQY) values in the solid state.[6] This is generally due to aggregation caused quenching (ACQ)[7] an effect that is often considerable in NIR emitting materials as the prerequisite low band-gap is typically achieved through the incorporation of extended planar π-systems and/or strongly electron donating and withdrawing units. These structural features generally promote aggregation which can induce alternative non-radiative decay processes.[8] Whilst the majority of NIR emissive materials developed to date are based on small molecules the development of conjugated polymer NIR emitters is highly desirable for facilitating solution processing of organic electronic devices and for generating dye-loaded polymer nanoparticles for bio-imaging applications that are stable to leakage of the NIR emitter.[9] However, effective NIR emissive polymers are rare and those reported to date generally contain transition metal complexes, complex repeat units (undesirable from a cost and/or toxicity perspective) and / or low percentages of the NIR chromophore (to minimize ACQ) thereby reducing the signal to background fluorescence ratio in the NIR region.[1,2,10]

To apply these NIR emitting polymers for *in vivo* imaging they need to be dispersed in water as conjugated

polymer nanoparticles (CPNPs).[11-17] CPNPs are highly desirable due to their low cost and low toxicity, particularly relative to heavy atom based emitters (e.g., CdSe quantum dots).[18] Fluorophores that have both high absorbance and good emission in the spectral region between 650 and 1500 nm are essential for *in-vivo* imaging as this region allows for greater photon penetration depths in mammalian tissue (millimetre versus micrometre with visible light).[4,19] An ideal agent for biomedical imaging should absorb in the deep red (or longer λ), have a large Stokes shift, emit in the NIR region of the spectrum with high PLQY values, have good photostability, be non-toxic, and stable in biological fluids.[20,21] In contrast, the most widely used NIR emitters (such as the FDA approved dye indocyanine green (ICG)) have relatively low brightness, small Stokes shifts and limited photostability.[22] Developing improved NIR imaging agents is therefore an important current challenge and herein we report a new family of NIR emitting polymers that meet many of the requirements outlined above. Electrophilic C-H borylation is used as a facile procedure to modify BT containing polymers, such as poly(9,9-dioctylfluorene-alt-benzothiadiazole) (PF8-BT), and this results in a substantial reduction of the polymer band-gap (by over 0.5 eV). The borylated F8-BT polymers have large Stokes shifts, and are highly efficient NIR emitters with emission λ_{max} values of ≥700 nm and solid state PLQY values up to 44%. Efficient solution processed NIR OLED devices and highly emissive, photostable CPNPs are constructed from these polymers. In phantom mouse studies the latter show superior signal to background ratios (SBR) for emission at 820 nm relative to ICG.

RESULTS AND DISCUSSION

Synthesis of P1-4. Electrophilic C-H borylation of BT containing small molecules by the addition of BCl_3 and subsequent functionalization at boron using diarylzinc reagents has been previously reported by several of us to produce highly emissive low band-gap small molecules.[23-27] The C-H functionalization methodology can be extended to PF8-BT (Mn 41 kDa, Mw 89 kDa, in THF at 35°C) and the percentage of borylated F8-BT NIR chromophore units incorporated into the polymer can be simply controlled by varying the molar equivalents of BCl_3 used (with respect to the repeat unit) followed by the addition of $ZnPh_2$. This results in the high yielding synthesis (>95%) of partially borylated **P1-3** (10, 15, and 25% borylation, Figure 1, top) and fully borylated PF8-BT, **P4**, functionalized with C,N-chelated BPh_2 groups. These are all highly stable to protic species and are thermally stable to >300 °C. It should be noted that post-polymerisation borylation produces a regio-irregular polymer (each fluorene unit could contain either 0, 1 or 2 boryl groups, see Scheme S1). However, we have previously shown that both types of borylated units have similar low LUMO energies.[23]

Electrochemical Properties. Cyclic voltammograms (CVs) of **P1-3** all show two reduction waves, a major reversible wave associated with the unborylated F8-BT units and an additional minor reduction wave at a significantly less negative reduction potential (by >0.5 eV) associated with the lower LUMO energy borylated F8-BT units (Figures S20 and S21). In the maximum borylated polymer **P4** only a single reduction wave is

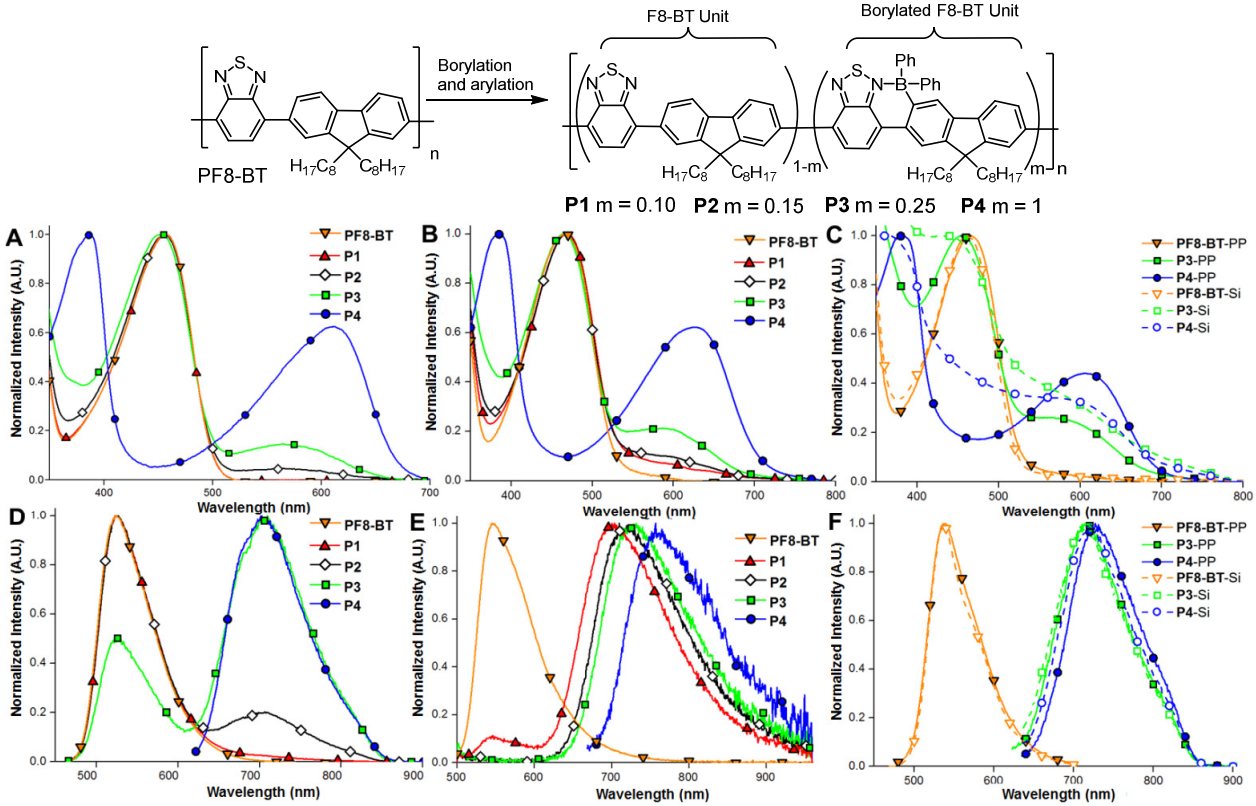

Figure 1. Top, synthesis of **P1-4**. Bottom, UV-vis absorbance of PF8-BT and borylated polymers A) in toluene (1 x 10^{-5} M), B) as thin films, C) encapsulated into CPNPs (PP-CPNPs and Si-CPNPs at 7.5 μg/ml). Emission of PF8-BT and borylated polymers, D) in toluene (1 x 10^{-5} M), E) as thin films, F) encapsulated into CPNPs (PP-CPNPs and Si-CPNPs at 7.5 μg/ml.

observed which is associated with the borylated units (Figure S23).Post-polymerization modification is particularly attractive as it removes the need to synthesize and polymerize borylated monomers,[28,29] and therefore represents a facile method to significantly reduce the band-gap of PF8-BT from ~2.60 eV for PF8-BT to 1.94 eV post C-H borylation by principally altering the LUMO energy.

Photophysical Properties. Photophysical studies confirm a low band-gap for these polymers, which is in the region of 1.9 eV from the onset of absorption for **P2-P4** (see tables S2 – S6). It is noteworthy that the absorbance spectra of **P1-3** in toluene solution shows absorption bands (~370-510 nm), associated with the unborylated F8-BT units, the intensity of which decreases as borylation level increases (Figure 1A and table S2). Concomitantly, the absorbance band associated with the borylated F8-BT units (520 to 650 nm) increases in absorption intensity on increasing the proportion of borylated chromophores. Upon exciting **P2** in dilute solution intense photoluminescence from the unborylated F8-BT units (emission λmax = 527 nm) is observed with only a minor amount of emission from the borylated units (emission λmax = 706 nm). Conversely, **P3** shows the majority of the emission from the borylated units (emission λmax = 710 nm) and minor emission from the F8-BT units. The maximum borylated polymer **P4** shows no observable optical features associated with unborylated F8-BT units (Figure 1A) and in toluene **P4** shows a considerable Stokes shift of (~100 nm) with a emission λmax at ~702 nm with a high (for fluorophores with emission λmax >700 nm) PLQY value of 12%.[6]

For organic electronic devices and when dispersed as CPNPs in water the solid state absorbance/emission characteristics of the polymers are more relevant. Polymers **P1-P4** show very similar trends in absorbance to those in solution but are red shifted (Figure 1A and B). In contrast, the solid state PL spectra of the borylated polymers (Figure 1E) differed drastically from those recorded in toluene solution (Figure 1D). When **P1** is excited at 468 nm in the solid state, the emission from the F8-BT units is almost completely absent with the majority of emission observed with an emission λmax of 700 nm and an exceptionally high (for deep red/NIR emitters) solid state PLQY of 44%. Emission from the unborylated F8-BT units is completely quenched in the solid state upon increasing the borylation level above 10% (**P2-4**) due to the increased concentration of borylated units in the polymer chain leading to an increased probability of energy transfer to the lower band-gap chromophore units. A progressive red shift in emission upon increasing the borylation level was observed with a solid state emission λmax of 700 nm for **P1** (PLQY = 44%), 710 nm for **P2** (PLQY = 32%), 731 nm for **P3** (PLQY = 23%), and the largest red shift is observed in the fully borylated polymer **P4** with a emission λmax value of 757 nm (PLQY = 11%). Whilst the solid state PL of all four polymers is high that of **P4** is particularly notable as it red shifted by >200 nm relative to PF8-BT, and the PLQY value of 11% at 757 nm is extremely high for organic fluorophores emitting in the solid state with a emission λmax >750 nm.[6] Furthermore, there is a significant Stokes shift (≥130 nm) in all these polymers whilst lifetime measurements revealed only prompt fluorescence (τ = <10 ns).

OLED Devices. With an appropriate spectral overlap to realise efficient energy transfer between PF8-BT and the borylated polymers PL studies on polymer blends were performed. This revealed excellent PLQY values, for example, upon excitation at 468 nm (optimal for unborylated PF8-BT) **P2** and **P3** blended with PF8-BT showed excellent PLQY values for solid state emission with λmax >700 nm (emission λmax = 715 nm and PLQY = 32-35%, Figure S18). Based on these promising results, solution processed deep red/NIR emitting OLEDs were fabricated using the borylated polymers (neat or as blends with PF8-BT) as the emissive layer. These devices were fabricated with the following architecture, ITO (45 nm) / Plexcore OC® AQ1200 (65 nm) / PF8-TFB (poly[(9,9-dioctylfluorenyl-2,7-diyl)-co-(4,4'-(N-(4-sec-butylphenyl)diphenyl amine))]) (22 nm) / emission layer (EML) (100 nm) / Ba (4 nm) / Al (100 nm) / Ag (100 nm). Devices with the EML consisting of neat films of **P1** (Device 1) and **P3** (Device 2) showed EQE_{max} values of 0.18 and 0.41%, respectively with both devices showing low EQE roll off at high current densities (EQE at 100 mA cm^{-2}: Device 1 = 0.17%, Device 2 = 0.26%). OLED devices were not fabricated from **P4** due to its poor surface wetting and film forming properties. The electroluminescence emission λmax values (λmax_{EL}) of Devices 1 and 2 were 688 and 716 nm, respectively (Fig. 2). The EQE_{max} value for **P3** is amongst the highest reported for non-doped solution processed, fluorescent OLEDs with a λmax_{EL} >700 nm, particularly with such a simple device structure.[6]

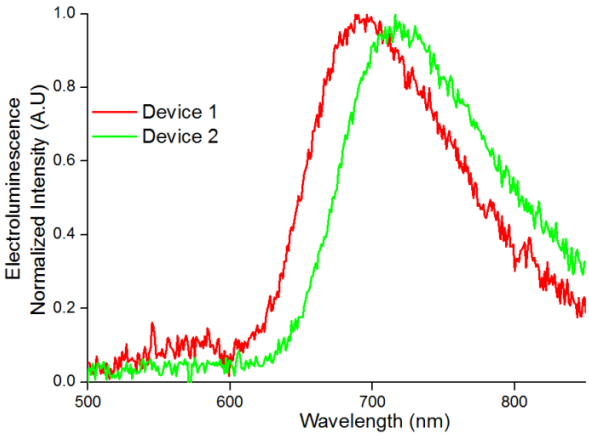

Figure 2. Electroluminescence spectra of devices 1 and 2.

CPNP Properties. The incorporation of a high percentage of NIR chromophore units in **P3** and **P4** leads to an appreciable absorbance in the deep red and excellent solid state emission in the NIR and suggests that these polymers are well-suited for use as in-vivo biological imaging agents. By contrast polymers **P1** and **P2** do not absorb significantly at λ >600 nm and are therefore not capable of excitation using photons in the spectral region required for deep tissue penetration. Recently, green emitting PF8-

BT has been encapsulated within diblock-copolymer CPNPs consisting of PEG-PLGA (PP)[30,31] or silica/Pluronic® F127 (Si) CPNPs.[32,33] Using an analogous approach **P3** and **P4** were encapsulated into either core shell PP or Si-CPNPs in which the conjugated polymer made up 5% and 1.4% of the theoretical CPNP mass, respectively. For both **P3** and **P4** systems, PP-CPNPs were larger than Si-CPNPs (~130 vs 30 nm) and were typically more polydisperse (Figure 3).

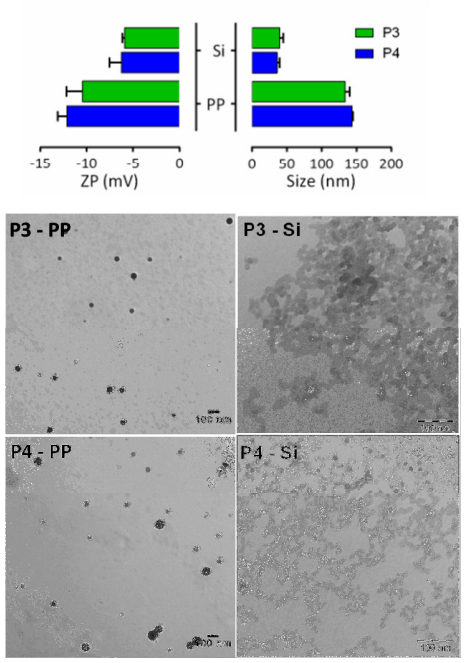

Figure 3. Top attributes of PP and Si-CPNP containing **P3** or **P4**, left Zeta potential (ZP) and right hydrodynamic diameter (mean ± standard deviation (SD), n=3 CPNP replicates). Bottom TEM micrographs of representative CPNPs

The photophysical properties of the **P3** and **P4** polymers in the core shell CPNPs suspended in aqueous solution were comparable to those observed in the thin films, albeit with a slight blue shift in the emission. Nevertheless, all emission maxima are >710 nm and quantum yields remain excellent for emission in the NIR region of the spectrum (PLQY values (emission maxima) P3-PP = 14% (714 nm), P4-PP = 6% (727 nm), P3-Si = 16% (717 nm) and P4-Si = 12% (721 nm)) with the majority of emission being > 700 nm (Figure 1F). Importantly, all four CPNPs showed excellent photophysical and colloidal stability for up to 20 days in suspension (Figure S27). As intravenous injection is a likely administration route for clinical diagnostic applications, haemocompatibility studies were performed over a concentration of 3-300 µg/mL total CPNP solids concentration (Figure 4). Significant haemolytic activity was observed only for the PP-CPNPs at the highest concentration tested. According to Dobrovolskaia et al.[34] in-vitro haemolysis assay values >50% of the positive control are often associated with possible clinical complications, while values <25% typically denote no clinical concerns, thus all concentrations of P3-Si and P4-Si meet this criteria. Furthermore, nanoparticle-induced platelet aggregation was not observed in this study, suggesting good biocompatibility (Figure 4).

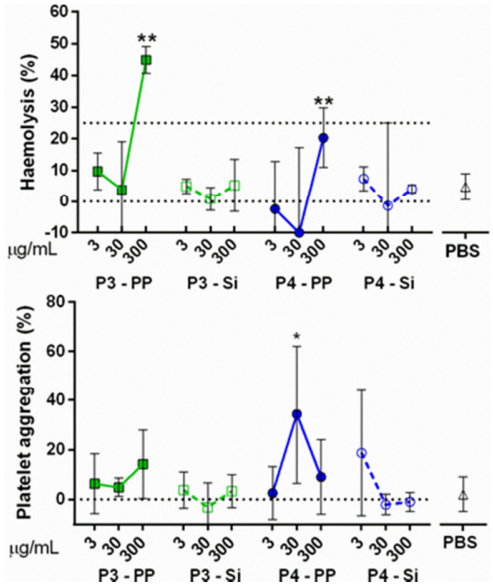

Figure 4. Top, Percentage erythrocyte haemolysis and bottom platelet aggregation (mean ± standard deviation, n=3 donors, *P<0.05, **P<0.01). 100% haemolysis was defined as the amount of haemoglobin release following treatment with poly-L-lysine, while 100% aggregation was defined as the turbidity value following treatment with adenosine diphosphate. Vehicle controls consisted of phosphate buffered saline (PBS).

Phantom Mouse Studies. To quantitatively compare the performance of the borylated polymer CPNPs with ICG for bioimaging applications, a phantom mouse with autofluorescence and light-scattering properties matching those of mouse muscle tissue was used. A 10 µL sample containing equivalent fluorophore masses (and therefore variable total solids concentrations) was pipetted into a silicon tube and placed inside the phantom at two depths (ventral = 4.0 mm and dorsal = 17.0 mm). The signal:background ratio (SBR) of the fluorescence signal (total radiant efficiency of sample = ROI1) to autofluorescence background (total radiant efficiency of background = ROI2) was calculated from identically sized regions of interest (ROI) and defined as (ROI1-ROI2)/ROI2.[35] Maximum SBR values for CPNP systems containing **P3** and **P4** were observed for the excitation and emission wavelengths of 640 / 820 nm, respectively, while ICG was imaged using a wavelength combination of 745 / 820 nm (Figure 5A/B). A linear increase in SBR values was observed for all CPNPs over a fluorophore mass range of 0.125 – 1 µg. CPNPs containing **P4** showed substantially higher SBR values compared to those of **P3** at all concentrations and tissue thicknesses, while Si-CPNP generally showed a slightly enhanced performance compared to PP-CPNP (Figure 5, right). Solutions of ICG in distilled water were non-linear over the concentration range tested and were outperformed by **P4** systems at all concentrations bar one. Thus P4-Si CPNPs combine the desirable properties of a simple high yielding preparation procedure (P4-Si CPNPs are produced in >90% yield), low toxicity, high photostability, a large Stokes shift, good quantum yield, high brightness for emission in the NIR when excited in the deep red region of the spectrum and a signal to background ratio for emission at 820 nm that outperforms ICG in tissue studies.

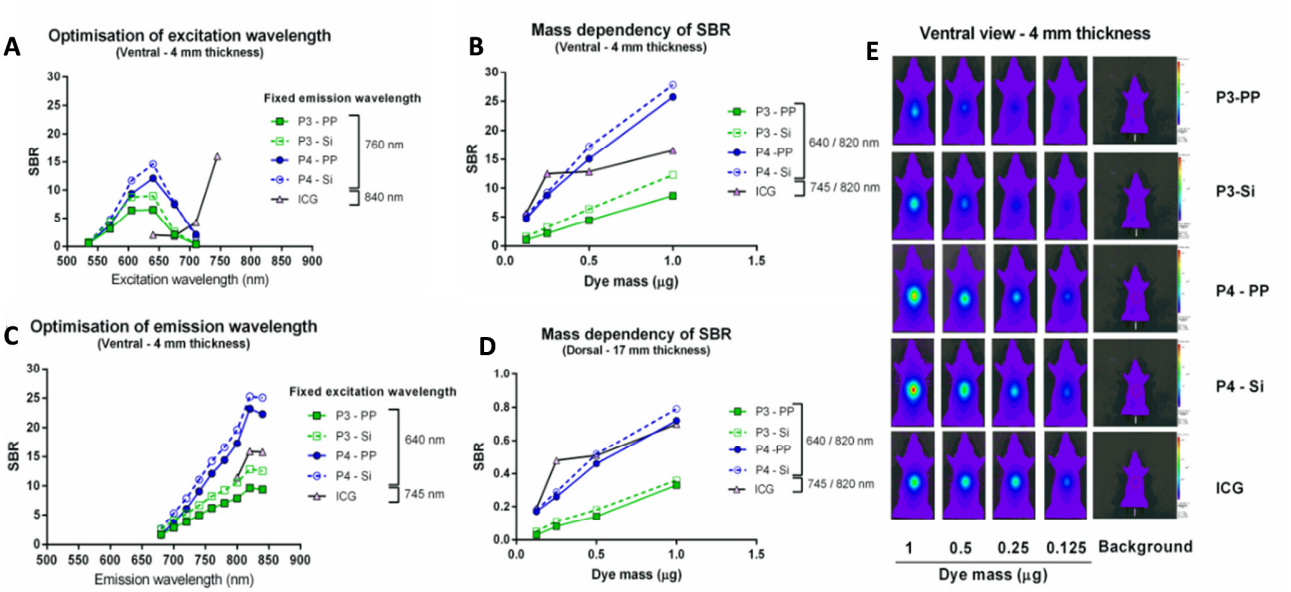

Figure 5. Imaging performance in a phantom mouse. Determination of maximal SBR over a range of excitation (A) and emission (B) wavelengths. SBR values for systems containing 0.125 – 1 µg fluorophore (in 10 µL) measured from the ventral (C) and dorsal (D) positions. E = representative images of signal patterns in a phantom mouse viewed from the ventral side. The color scales show total radiant efficiency values ([photon/s/cm²/steradian]/[µW/cm²]) ranging from 7.44 x10^5 (blue) to 6.34 x10^8 (red).

Borylation of PF8TBT. With the utility of post-polymerization C-H borylation as a method to significantly reduce the band gap established on PF8-BT we next sought to demonstrate the extension of this methodology to other polymers. Therefore the C-H borylation of poly((9,9-dioctylfluorene)-2,7-diyl-alt-[4,7-bis(3-hexylthien-5-yl)-2,1,3-benzothiadiazole]-2c,2cc-diyl) (PF8TBT), a donor acceptor polymer which has been studied in a range of optoelectronic devices, was investigated.[36,37] PF8TBT requires C-H borylation of a thiophene moiety instead of fluorene and was chosen as it is a potentially challenging polymer to borylate due to the sterically hindered environment around the borylation position of the thiophene (which has an *ortho*-hexyl chain).[38,39] After the addition of excess BCl_3 to PF8TBT (Mn 47 kDa, Mw 85 kDa) NMR spectroscopy (Figure S8-10) confirmed that significant C-H functionalization has proceeded. Subsequent degassing and functionalization with $AlMe_3$ enabled the resultant borylated polymer (**P5**, scheme 1) to be isolated with > 95 % C-H borylation level with the polymer stable to ambient atmosphere and wet (non-purified) solvents. The synthesis of **P5** demonstrates that post borylation the boron centre can be functionalized with alkyl groups equally readily to aryl (as used with PF8-BT) further increasing the scope of this methodology. Importantly, a significant reduction in the optical band-gap of the borylated polymer **P5** relative to PF8TBT was observed (optical band gap reduced from 2.07 to 1.65 eV, $\Delta E = 0.42$ eV) in addition to a considerable red-shift in the photoluminescence emission maximum which changes from 655 nm for PF8TBT to 810 nm for **P5** (measured as dilute DCM solutions see Figure S19). Therefore this post polymerization C-H functionalization method is a simple and general procedure for modulating the band gap and emission properties of common donor acceptor polymers. It is particularly useful for generating low band gap materials that are emissive in the NIR region of the spectrum.

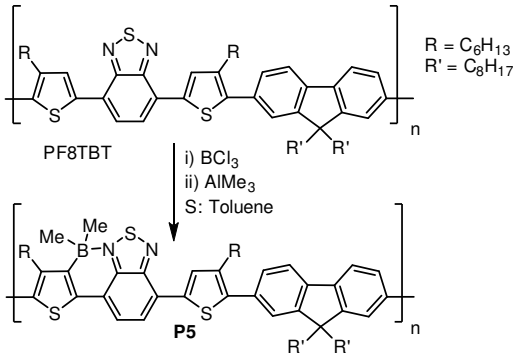

Scheme 1. Synthesis of **P5**

CONCLUSION

In conclusion, post-polymerization modification by C-H electrophilic borylation is a simple and general high yielding method to introduce controlled concentrations of low band-gap chromophores into conjugated polymer main chains and red shift the emission by >150 nm relative to the pristine polymers. These polymers possess large Stokes shifts and exhibit extremely strong photoluminescence in the solid state with absolute PLQY values up to 44% in the far red/NIR region of the electromagnetic spectrum. Unoptimized solution processed OLED devices with the emission layer comprised of neat films of the borylated polymers showed good EQE_{max} values for simple non-doped solution processed devices in the NIR region of the electromagnetic spectrum. It is also noteworthy that polymers containing higher borylation levels demonstrated red shifted EL and superior EQE values.

Core shell CPNPs with encapsulated borylated polymers exhibited excellent colloidal and photophysical properties that are suitable for in vivo imaging applications. In phantom mouse studies these CPNPs outperformed the ubiquitous NIR dye, indocyanine green, across a range of dye loadings. We are currently investigating a variety of other low band-gap borylated BT-polymers for a range of applications.

ASSOCIATED CONTENT

Supporting Information. The Supporting Information is available free of charge on the ACS Publications website at DOI: xx.xxxx/acsami.xxxxxxx.
Experimental details, characterization of nanoparticles, NMR spectra, TGA plots, DSC plots, OLED data, CVs. GPCs (PDF)

AUTHOR INFORMATION

Corresponding Authors

E-mail: michael.ingleson@manchester.ac.uk

E-mail: michael.turner@manchester.ac.uk

E-mail: lea.dailey@pharmazie.uni-halle.de

ACKNOWLEDGMENT

The research leading to these results has received funding from Cambridge Display Technology Limited (Company Number 02672530, CDT/EPSRC Case Award to D.L.C.) the EPSRC (EP/K03099X/1 and EP/K018876/1) and the European Research Council (FP/2007–2013/ERC Grant Agreement 305868 and Proof of Concept Grant 713368). M.J.I. acknowledges the Royal Society (for the award of a University Research Fellowship) and M.L.T. thanks InnovateUK for financial support of the Knowledge Centre for Material Chemistry. Carl Alberto Lorenzon and Moritz Schüller are also thanked for assistance.

REFERENCES

(1) Dou, L.; Liu, Y.; Hong, Z.; Li, G.; Yang, Y. Low-Bandgap Near-IR Conjugated Polymers/Molecules for Organic Electronics *Chem. Rev.* **2015**, 115, 12633-12665.

(2) Xiang, H.; Cheng, J.; Ma, X.; Zhou, X.; Churma, J. Near-infrared Phosphorescence: Materials and Applications *Chem. Soc. Rev*. **2013**, 42, 6128-6185.

(3) Qian, G.; Wang, Z. Y. Near-Infrared Organic Compounds and Emerging Applications *Chem. Asian. J*. **2010**, 5, 1006-1029.

(4) Hong, G.; Antaris, A.; Dai, H. Near-Infrared Fluorophores for Biomedical Imaging *Nat. Biomed. Eng*. **2017**, 1, 0010.

(5) Yu, J.; Rong, Y.; Kuo, C.-T.; Zhou, X.-H.; Chiu, D. T. Recent Advances in the Development of Highly Luminescent Semiconducting Polymer Dots and Nanoparticles for Biological Imaging and Medicine *Anal. Chem*. **2017**, 89, 42-56.

(6) Liu, T.; Zhu, L.; Zhong, C.; Xie, G.; Gong, S.; Feng, J.; Ma, D.; Yang, C. Naphthothiadiazole-Based Near-Infrared Emitter with a Photoluminescence Quantum Yield of 60% in Neat Film and External Quantum Efficiencies of up to 3.9% in Nondoped OLEDs *Adv. Funct. Mater.* **2017**, 27, 1606384 and references therein.

(7) Mei, J.; C. Leung, N. L.; Kwok, R. T. K.; Lam, J. W. Y.; Tang, B. Z. Aggregation-Induced Emission: Together We Shine, United We Soar *Chem. Rev*. **2015**, 115, 11718-11940.

(8) Lu, H.; Zheng, Y.; Zhao, Z.; Wang, L.; Ma, S.; Han, X.; Xu, B.; Tian, W.; Gao, H. Highly Efficient Far Red/Near-Infrared Solid Fluorophores: Aggregation-Induced Emission, Intramolecular Charge Transfer, Twisted Molecular Conformation, and Bioimaging Applications *Angew. Chem. Int. Ed*. **2016**, 55, 155-159 and references therein.

(9) Yu, J.; Wu, C.; Zhang, X.; Ye, F.; Gallina, M. E.; Rong, M. E.; Y.; Wu, I.-C.; Sun, W.; Chan, Y.-H.; Chiu, D. T. Stable Functionalization of Small Semiconducting Polymer Dots via Covalent Cross-Linking and Their Application for Specific Cellular Imaging *Adv. Mater*. **2012**, 24, 3498-3504.

(10) Freeman, D. M. E.; Minotto, A.; Duffy, W.; Fallon, K. J.; McCulloch, I.; Cacialli, F.; Bronstein, H. Highly Red-Shifted NIR Emission from a Novel Anthracene Conjugated Polymer Backbone Containing Pt(II) Porphyrins *Polym. Chem*. **2016**, 7, 722-730 and references therein.

(11) Chen, D.; Wu, I.; Liu, Z.; Tang, Y.; Chen, H.; Yu, J.; Wu C.; Chiu, D. T. Semiconducting Polymer Dots with Bright Narrowband Emission at 800 nm for Biological Applications *Chem. Sci*. **2017**, 8, 3390-3398.

(12) Wu, I. C.; Yu, J.; Ye, F.; Rong, Y.; Gallina, M. E.; Fujimoto, B. S.; Zhang, Y.; Chan, Y.; Sun, W.; Zhou, X. H.; Wu, C.; Chiu, D. T. Squaraine-Based Polymer Dots with Narrow, Bright Near-Infrared Fluorescence for Biological Applications *J. Am. Chem. Soc*. **2014**, 137, 173-178.

(13) Zhang, X.; Yu, J.; Rong, Y.; Ye, F.; Chiu, D. T.; Uvdal, K. High-Intensity Near-IR Fluorescence in Semiconducting Polymer Dots Achieved by Cascade FRET Strategy *Chem. Sci*. **2013**, 4, 2143-2151.

(14) Liu, H. Y.; Wu, P. J.; Kuo, S. Y.; Chen, C. P.; Chang, E. H.; Wu, C. Y.; Chan, Y. H. Quinoxaline-Based Polymer Dots with Ultrabright Red to Near-Infrared Fluorescence for In Vivo Biological Imaging *J. Am. Chem. Soc*. **2015**, 137, 10420-10429.

(15) Zhu, H.; Fang, Y.; Zhen, X.; Wei, N.; Gao, Y.; Luo, K. Q.; Xu, C.; Duan, H.; Ding, D.; Chen, P.; Pu, K. Multilayered Semiconducting Polymer Nanoparticles with Enhanced NIR Fluorescence for Molecular Imaging in Cells, Zebrafish and Mice *Chem. Sci*. **2016**, 7, 5118-5125.

(16) Chen, C.-P.; Huang, Y.-C.; Liou, S.-Y.; Wu, P.-J.; Kuo, S.-Y.; Chan, Y.-H. Near-Infrared Fluorescent Semiconducting Polymer Dots with High Brightness and Pronounced Effect of Positioning Alkyl Chains on the Comonomers *ACS Appl. Mater. Interfaces* **2014**, 6, 21585-21595.

(17) Liu, J.; Chen, C.; Ji, S.; Liu, Q.; Ding, D.; Zhao, D.; Liu, B. Long Wavelength Excitable Near-Infrared Fluorescent Nanoparticles with Aggregation-Induced Emission Characteristics for Image-Guided Tumor Resection *Chem. Sci*. **2017**, 8, 2782-2789 and references therein.

(18) Tsoi, K. M.; Dai, Q.; Alman, B.; Chan, W. C. W. Are Quantum Dots Toxic? Exploring the Discrepancy Between Cell Culture and Animal Studies *Acc. Chem. Res*. **2013**, 46, 662-671.

(19) Yu, J.; Zhang, X.; Zhang, X. H. X.; Zhou, M.; Lee, C. S.; Chen, X. Near-Infrared Fluorescence Imaging using Organic Dye Nanoparticles *Biomaterials* **2014**, 35, 3356-3364.

(20) Khanbeigi, R. A.; Abelha, T. F.; Woods, A.; Rastoin, O.; Harvey, R. D.; Jones, M.-C.; Forbes, B.; Green, M.; Collins, H.; Dailey, L. A. Surface Chemistry of Photoluminescent F8BT Conjugated Polymer Nanoparticles Determines Protein Corona Formation and Internalization by Phagocytic Cells *Biomacromolecules* **2015**, 16, 733-742.

(21) Khanbeigi, R. A.; Hashim, Z.; Abelha, T. F.; Pitchford, S.; Collins, H.; Green, M.; Dailey, L. A. Interactions of Stealth Conjugated Polymer Nanoparticles with Human Whole Blood *J. Mat. Chem. B* **2015**, 3, 2463-2471.

(22) Ke, C.-S.; Fang, C.-C.; Yang, J.-Y.; Tseng, P.-J.; Pyle, J. R.; Chen, C. P.; Lin, S. Y.; Chen, J.; Zhang, X.; Chan, Y.-H. Merging Single-Atom-Dispersed Silver and Carbon Nitride to a Joint Electronic System via Copolymerization with Silver Tricyanomethanide *ACS Nano* **2017**, 11, 3166-3175.

(23) Crossley, D. L.; Cade, I. A.; Clark, E. R.; Escande, A.; Humphries, M. J.; King, S. M.; Vitorica-Yrezabal, I.; Ingleson, M. J.; Turner, M. L. Enhancing Electron Affinity and Tuning Band gap in Donor–Acceptor Organic Semiconductors by Benzothiadiazole Directed C–H Borylation *Chem. Sci*. **2015**, 6, 5144-5151.

(24) Crossley, D. L.; Vitorica-Yrezabal, I.; Humphries, M. J.; Turner, M. L.; Ingleson. M. J. Highly Emissive Far Red/Near-IR Fluorophores Based on Borylated Fluorene–Benzothiadiazole Donor–Acceptor Materials *Chem. Eur. J*. **2016**, 22, 12439-12448.

(25) Yusuf, M.; Liu, K.; F.; Guo, R.; Lalancette, A.; Jäkle, F. Luminescent Organoboron Ladder Compounds via Directed Electrophilic Aromatic C–H Borylation *Dalton Trans*. 2016, 45, 4580-4587.

(26) Zhu, C.; Guo, Z.-H.; Mu, A. U.; Liu, Y.; Wheeler, S. E.; Fang, L. J. Low Band Gap Coplanar Conjugated Molecules Featuring Dynamic Intramolecular Lewis Acid–Base Coordination *J. Org. Chem*. 2016, 81, 4347-4352.

(27) Ishida, N.; Moriya, T.; Goya, T.; Murakami, M. Synthesis of Pyridine–Borane Complexes via Electrophilic Aromatic Borylation *J. Org. Chem*. **2010**, 75, 8709-8712.

(28) Dou, C.; Ding, Z. Zhang, Z.; Xie, Z.; Liu, J.; Wang, L. Developing Conjugated Polymers with High Electron Affinity by Replacing a C-C unit with a B←N Unit *Angew. Chem. Int. Ed*. **2015**, 54, 3648-3652.

(29) Zhang, Z.; Ding, Z.; Dou, C.; Liu, J.; Wang, L. Development of a Donor Polymer Using a B ← N Unit for Suitable LUMO/HOMO Energy Levels and Improved Photovoltaic Performance *Polym. Chem*. **2015**, 6, 8029-8035.

(30) Abelha, T. F.; Phillips, T. W.; Bannock, J. H.; Nightingale, A. M.; Dreiss, C. A.; Kemal, E.; Urbano, L.; Demello, J. C.; Green, M.; Dailey, L. A. Bright Conjugated Polymer Nanoparticles Containing a Biodegradable Shell Produced at High Yields and with Tuneable Optical Properties by a Scalable Microfluidic Device *Nanoscale* **2017**, 9, 2009-2019.

(31) Kemal, E.; Abelha, T. F.; Urbano, L.; Peters, R.; Owen, D. M.; Howes, P.; Green, M.; Dailey, L. A. Bright, Near Infrared Emitting PLGA–PEG Dye-Doped CN-PPV Nanoparticles for Imaging Applications *RSC Adv*. **2017**, 7, 15255-15264.

(32) Geng, J.; Goh, C. C.; Tomczak, N.; Liu, J.; Liu, R.; Ma, L.; Ng, L. G.; Gurzadyan, G. G.; Liu, B. Micelle/Silica Co-protected Conjugated Polymer Nanoparticles for Two-Photon Excited Brain Vascular Imaging *Chem. Mater*. **2014**, 26, 1874-1880.

(33) Huo, Q. S.; Liu, J.; Wang, L. Q.; Jiang, Y. B.; Lambert, T. N.; Fang, E. A New Class of Silica Cross-Linked Micellar Core–Shell Nanoparticles *J. Am. Chem. Soc*. **2006**, 128, 6447-6453.

(34) Dobrovolskaia, M. A.; Clogston, J. D.; Neun, B. W.; Hall, J. B.; Patri, A. K.; McNeil, S. E. Method for Analysis of Nanoparticle Hemolytic Properties In Vitro *Nano Lett*. **2008**, 8, 2180-2187.

(35) Shcherbakova, D. M.; Verkhusha, V. V. Near-infrared Fluorescent Proteins for Multicolor *In Vivo* Imaging *Nat. Methods* **2013**, 10, 751-754.

(36) McNeill, C. R.; Abrusci, A.; Zaumseil, J.; Wilson, R.; McKiernan, M. J.; Burroughes, J. H.; Halls, J. J.; M.; Greenham, N. C.; Friend R. H. Dual Electron Donor/Electron Acceptor Character of a Conjugated Polymer in Efficient Photovoltaic Diodes *Appl. Phys. Lett*. **2007**, 90, 193506.

(37) Lu, L.; Finlayson, C.; Kabra, D.; Albert-Seifried, S.; Song, M.; Havenith, R.; Tu, G.; Huck, W.; Friend, R. The Influence of Side-Chain Position on the Optoelectronic Properties of a Red-Emitting Conjugated Polymer *Macromol. Chem. Phys*. **2013**, 214, 967-974.

(38) Bagutski, V.; Del Grosso, A.; Ayuso Carrillo, J.; Cade, I. A.; Helm, M. D.; Lawson, J. R.; Singleton, P. J.; Solomon, S. A.; Marcelli, T.; Ingleson, M. J. Mechanistic Studies into Amine-Mediated Electrophilic Arene Borylation and Its Application in MIDA Boronate Synthesis *J. Am. Chem. Soc*. **2013**, 135, 474-487.

(39) Attempts to C-H borylate a more hindered polymer pCPDT-BT using BBr_3 led only to BBr_3 coordination to BT and no C-H functionalization, see: Welch, G. C.; Bazan, G. C. Lewis Acid Adducts of Narrow Band Gap Conjugated Polymers *J. Am. Chem. Soc*. **2011**, *133*, 4632-4644.

TOC Graphic:

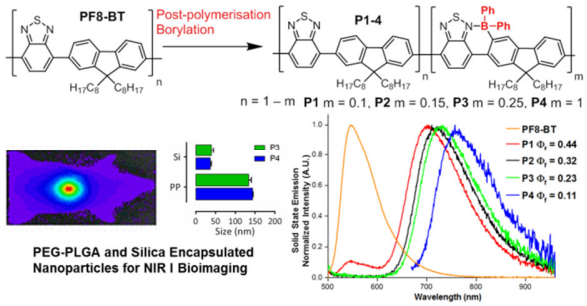
PF8-BT
Post-polymerisation
Borylation
P1-4
Ph
B–Ph
n = 1 – m P1 m = 0.1, P2 m = 0.15, P3 m = 0.25, P4 m = 1
Si
PP
P3
P4
0 50 100 150 200
Size (nm)
PEG-PLGA and Silica Encapsulated
Nanoparticles for NIR I Bioimaging
Solid State Emission
Normalized Intensity (A.U.)
Wavelength (nm)
PF8-BT
P1 Φf = 0.44
P2 Φf = 0.32
P3 Φf = 0.23
P4 Φf = 0.11